

## Electronically induced defect creation at semiconductor/oxide interface revealed by time-dependent density functional theory


Yue-Yang Liu<sup>1,2</sup>, Zhongming Wei,<sup>1</sup> Sheng Meng,<sup>3,\*</sup> Runsheng Wang,<sup>4</sup> Xiangwei Jiang,<sup>1,†</sup> Ru Huang,<sup>4</sup> Shu-Shen Li,<sup>1</sup> and Lin-Wang Wang<sup>2,‡</sup>

<sup>1</sup>State Key Laboratory of Superlattices and Microstructures, Institute of Semiconductors, Chinese Academy of Sciences, Beijing 100083, China

<sup>2</sup>Materials Sciences Division, Lawrence Berkeley National Laboratory, Berkeley, California 94720, USA

<sup>3</sup>Beijing National Laboratory for Condensed Matter Physics and Institute of Physics, Chinese Academy of Sciences, Beijing 100190, China

<sup>4</sup>Institute of Microelectronics, Peking University, Beijing 100871, China

 (Received 9 March 2021; revised 24 June 2021; accepted 13 September 2021; published 30 September 2021)

Carrier induced defect creation at the semiconductor-oxide interface has been known as the origin of electronic device degradation for a long time, but how exactly the interface lattice can be damaged by carriers (especially low-energy ones) remains unclear. Here we carry out real-time time-dependent density functional theory simulations on concrete Si/SiO<sub>2</sub> interfaces to study the interaction between excited electrons and interface bonds. We show that the normal interface Si-H bonds are generally resistant to electrons due to the delocalized nature and high energy level of the Si-H antibonding states, and due to the high-energy barrier to break the Si-H bond. However, if an additional hydrogen atom exists by attaching to a nearby oxygen atom (forming a “Si-H···H-O” complex), the Si-H bond will be greatly weakened, including the reduction of energy barrier for bond breaking, and the lowering of the antibonding state energy level which favors electron injection. Together with the multiple vibrational excitation process, the corresponding Si-H bond can be broken much more easily. Thus we propose that the Si-H···H-O complex will be the center for defect creation and device degradation. We also explain why such a center might be relatively easy to form during the hydrogen annealing process.

DOI: [10.1103/PhysRevB.104.115310](https://doi.org/10.1103/PhysRevB.104.115310)

### I. INTRODUCTION

Hydrogens have been introduced to silicon-based semiconductor devices intentionally with the mission to terminate dangling bonds, remove gap states, and relax surface strains. However, hydrogen treatment does not provide a permanent solution due to the breaking of the Si-H bonds during device operation, which brings the charge trapping centers back and causes device degradations [1–4]. The desire to solve such device reliability issues has been driving people to study Si-H bond stability and kinetics for decades [5–14]. In another area, the scanning tunneling microscopy (STM) study of hydrogen desorption from the Si surface has also promoted the study of Si-H bond dissociation for many years [15–19].

The bond breaking phenomenon in devices used to be attributed to the high energy (hot) of the channel carriers, but question and controversy arose after failing to solve the problem by reducing the operation voltage to as low as  $\approx 1$  eV in ultrascaled metal-oxide-semiconductor field-effect transistors (MOSFETs) [20–22]. It was then realized that the low-energy (cold) carriers could also damage the semiconductor-oxide interface in some unknown way. The prevailing explanation of the phenomenon is twofold. One is that the electron-electron scattering effect can populate the high-energy fraction of the

carrier ensemble [23–25], and the other is that even low-energy electrons can excite the Si-H bond vibration [through multiple vibrational excitation (MVE)] until the bond accumulates enough energy to dissociate [15,26–30]. The MVE mechanism was proposed during investigations on hydrogen desorption from the Si surface, but was also recognized as the mechanism for Si-H bond breaking in MOSFETs following some experimental observations, e.g., the dependence of interface trap generation on current (electron) density and the significant hydrogen/deuterium isotope effect [26,27]. Nevertheless, these Si-H bond breaking mechanisms are still rough ideas that were very recently deemed to be “speculative” [31], and “more work is needed to understand it” [32]. Investigation and explanation of them at the atomic level are essential so that correct analytical frameworks for defect creation can be developed, and possible solutions could be proposed accordingly. On top of this, it has been tacitly accepted that the Si-H bond breaking is the whole picture of carrier induced interface defect creation [30–32], but whether Si-O bonds can also be broken by low-energy carriers has not been revealed. In short, the physical origin of defect creation at the semiconductor-oxide interface is far from understood. A deep insight into the interaction between nonequilibrium carriers and Si-H (Si-O) bonds in semiconductor-oxide interfaces, and the subsequent guidance to keep the bonds from breaking, is in urgent need as modern electronic devices get smaller and degradation becomes a major issue.

The challenge of studying defect creation is huge because it is a dynamical process that involves both electron excitation

\* smeng@iphy.ac.cn

† xwjjiang@semi.ac.cn

‡ lwwang@ibl.gov

and electron-phonon interaction, and simultaneously depends on the atomic environment of the interfaces. Therefore, we propose to use the *ab initio* time-dependent density functional theory (TDDFT) approach, which can take into account all the factors mentioned above, to study the carrier induced defect creation at Si/SiO<sub>2</sub> interfaces. By doing this, we demonstrate how the low-energy electrons can transfer energy to the Si-H bonds through multiple electron-bond interactions, but at the same time how difficult the process is. On the other hand, we reveal how the nearby H atom can assist cold carriers to break not only the Si-H bond but also the Si-O bond. These results provide deep understanding on the defect creation issue in semiconductor devices.

## II. SIMULATION DETAILS

The basic idea of TDDFT is to solve the time-dependent Schrödinger equation:

$$i \frac{\partial \psi_i(t)}{\partial t} = [\hat{T} + \hat{V}_{ee} + \hat{V}_{\text{ext}}(t)] \psi_i(t) \quad (1)$$

where the right-hand side three terms are kinetic energy, electron-electron interaction, and external potential, respectively. The zero-time wave functions are obtained by static self-consistent field (SCF) calculations on the initial system. After that, their occupations at  $t = 0$  are selectively changed to mimic certain instantaneous electron excitations. After that, the electron states will evolve with time following Eq. (1) while the nuclear positions  $R_j(t)$  will evolve with time following Newton's second law:

$$M_j d^2 R_j(t) / dt^2 = F_j(t), \quad (2)$$

in which  $M_j$  is the mass of atom  $j$ , and  $F_j$  is the *ab initio* force from the TDDFT calculation. In our approach [33,34], to integrate Eq. (1), the  $\psi_i(t)$  will be expanded with the basis of the adiabatic eigenstates  $\phi_l(t)$ :

$$\psi_i(t) = \sum_l C_{i,l}(t) \phi_l(t), \quad (3)$$

$$H[t, R_j(t), \rho(t)] \phi_l(t) = \varepsilon_l \phi_l(t). \quad (4)$$

Plugging Eqs. (3) and (4) into Eq. (1) gives the coefficients

$$\dot{C}_{i,l}(t) = -i\varepsilon_l(t)C_{i,l}(t) - \sum_k C_{i,k}(t)V_{lk}(t) \quad (5)$$

where  $V_{lk}(t) = \langle \phi_l(t) | \partial \phi_k(t) / \partial t \rangle$  is the coupling between adiabatic states  $l$  and  $k$ .

In this paper, the PWmat implemented in the PwMAT package optimized on GPU architecture is used [35,36]. All the calculations are carried out with SG15 norm-conserving pseudopotentials [37] and a cutoff energy of 50 Ry. The temperature is set to 300 K. Three kinds of models have been studied. The first model is a Si<sub>4</sub>H<sub>10</sub> cluster that is isolated in a box of  $15 \times 15 \times 15 \text{ \AA}$ . The second model is a crystalline-Si/amorphous-SiO<sub>2</sub> planar interface structure with 154 atoms and a supercell of  $11.52 \times 11.52 \times 24.24 \text{ \AA}$ . The third model is a crystalline-Si/amorphous-SiO<sub>2</sub> gate-all-around (GAA) structure, which contains 577 atoms, and the supercell is relaxed as  $24.86 \times 28.53 \times 11.65 \text{ \AA}$ . Such a GAA model

contains more local motifs at the interface than the planar one, and thus can better reflect the complicated interface in real devices. All the models are designed to be fully periodic so that there is no need to passivate the dangling bonds at the two sides of models by a lot of H atoms, the electronic states of which could degenerate with that of the interface H atom, and consequently influence the study on the interface Si-H bonds. The amorphous SiO<sub>2</sub> in each model is obtained by the Monte Carlo bond-switching method, which has been reported to be excellent in producing amorphous SiO<sub>2</sub> and yielding correct Si/SiO<sub>2</sub> band alignment [38]. At every step of the bond-switching simulation, two neighboring bonds (e.g., AC and BD) are randomly selected and broken, and then two new bonds (e.g., BC and AD) are formed in a valence bond model. The system with these new bonds will experience a structural relaxation, and whether the new structure will be accepted is decided by the METROPOLIS probability  $P = \min\{1, \exp[(E_i - E_f)/k_B T]\}$ , where  $E_i$  and  $E_f$  are the energy before and after bond switching, respectively. To make the structure fully amorphous, the system is put into a very high temperature (e.g., 10 000 K) at the beginning, and the first 250 steps are forced to accept. The total step is set to be  $\approx 260\,000$  with decreasing temperatures. Considering the large size of these supercells, the generalized gradient approximation-Perdew-Burke-Ernzerhof functional is adopted and only the Gamma point is sampled during the DFT simulations. To be prudent, the HSE functional has also been used to repeat the SCF calculations on the Si/SiO<sub>2</sub> interface, and accordant results are obtained (see Fig. S1 in the Supplemental Material [39]).

## III. RESULTS AND DISCUSSION

### A. Typical Si-H electronic states and bond dynamics

Before dealing with large Si/SiO<sub>2</sub> interfaces, we first take a look at a small Si<sub>4</sub>H<sub>10</sub> cluster, the top Si-H bond of which has a similar environment with that in the Si/SiO<sub>2</sub> interface. The electronic structure of the Si-H bond is analyzed by the partial density of states (PDOS) and the wave-function plot of each state. As shown in Fig. 1(a), there are two typical Si-H bonding states (4th and 11th) and two antibonding (AB) states (14th and 20th). The two occupied bonding states both have a wave-function bulb at the Si-H bond while the two empty AB states (Upper and Lower) differ greatly with each other in the wave-function shape. Such characteristic will be mentioned again in the Si/SiO<sub>2</sub> interface case. With these Si-H states identified, we can simulate the effect of electron excitation on Si-H bond vibration with TDDFT. The Si-H bond vibration at the ground state (black line) is shown in Fig. 1(b), from which we can see that the stretching vibration is nearly harmonic with an amplitude of  $\approx 0.036 \text{ \AA}$  and a periodicity of  $\approx 15.9 \text{ fs}$ , which is in good agreement with experimental values on the Si surface [40]. When an electron is excited from the bonding state (11th) to the lower AB state (14th) at 12 fs, a repulsive force as large as  $2.1 \text{ eV/\AA}$  is imposed on the H atom, and consequently the Si-H bond breaks rapidly without delay. It is worth mentioning that the Si-H bond will not break (blue line) if only one electron is injected to the AB state, indicating that a single electron injection has a much smaller effect

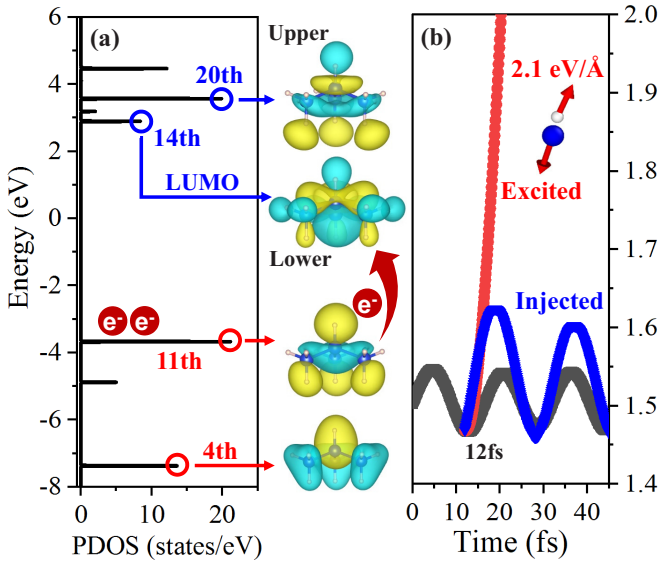


FIG. 1. (a) The partial DOS of the top H atom in a  $\text{Si}_4\text{H}_{10}$  molecule, and the wave function of each Si-H state. (b) The vibration of the Si-H bond at ground state (black), after electron injection (blue), and after electron excitation (red). The inset shows the large force caused by electron excitation.

than the electron excitation, where besides the electron at the antibonding state there is also a hole in the bonding state.

### B. Mutation of Si-H states and bond dynamics in a Si/SiO<sub>2</sub> interface

Following the same procedure, we study the Si-H states in a Si/SiO<sub>2</sub> interface, which is the key component of modern semiconductor devices. However, different from the case of the  $\text{Si}_4\text{H}_{10}$  cluster, the PDOS of the H atom at the Si/SiO<sub>2</sub> interface shows a broad distribution within a wide range of energies rather than isolated peaks, as shown in Fig. 2(a). This indicates that the Si-H states are no longer localized. The

wave functions of the states that correspond to the main PDOS peaks confirm this picture, as shown in Figs. 2(b) and 2(c). It can be seen that the Si-H states have been strongly mixed with some bulk Si states. Since the Si-H states are delocalized, they are not able to trap carriers like typical defects do [41–44]. This is a merit of H passivation, i.e., it destroys the localized defect states in band gaps. Moreover, it is seen from Fig. 2(a) that the energy difference between the main occupied Si-H states and the empty states is more than 5 eV, which means that the electron excitation from Si-H bonding states to Si-H AB states is unlikely in an ultrascaled MOSFET. Note, although the Si-H states will move towards the band edge with increasing bond length, the magnitude is rather small (see Fig. S2 in the Supplemental Material [39]), which will not change the high-energy position problem. Therefore, it should only be the transfer of free channel electrons to the empty Si-H states that causes Si-H bond breaking and hot/cold carrier degradation. To explore this possibility, we first ask the question: is there a correlation of these mixed Si-H states with the localized ones shown in the  $\text{Si}_4\text{H}_{10}$  cluster, given that their local Si-H bonding environments look similar? More importantly, how will the Si-H bond vibration behave when these mixed states are excited with electrons?

Considering that the mixed states could come from the coupling of Si-H states with some bulk Si states, it makes sense to find a way to decouple them back, i.e., by mixing the eigenstates  $\varphi_i(r)$  together:

$$\Phi(r) = \sum_i C_i \varphi_i(r). \quad (6)$$

The coefficients  $C_i$  can be obtained by requiring  $\Phi(r)$  to be localized around the Si-H bond. Inspired by the basic idea of constrained DFT [45], we utilize a local weight function  $[\omega_c(r)]$  obtained by the Becke partitioning scheme, and construct the following Lagrange function:

$$L = \int \omega_c(r) |\Phi(r)|^2 dr + \lambda \left( \sum_i C_i^2 - 1 \right), \quad (7)$$

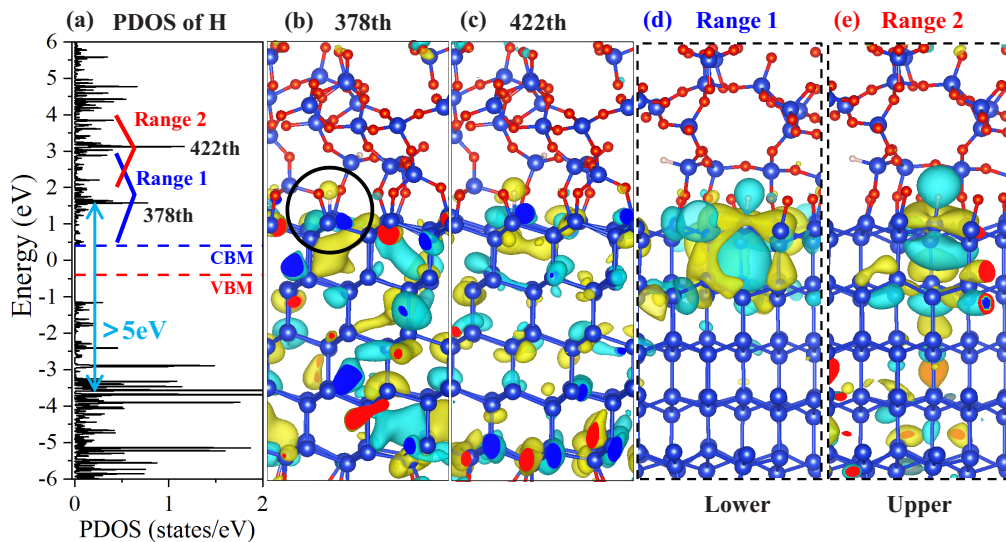


FIG. 2. (a) The PDOS of the H atom at the Si/SiO<sub>2</sub> interface. (b), (c) The wave function of the two Si-H states that correspond to the PDOS peaks. (d), (e) The decoupled Si-H states obtained by superposition of the eigenstates within range 1 and range 2.



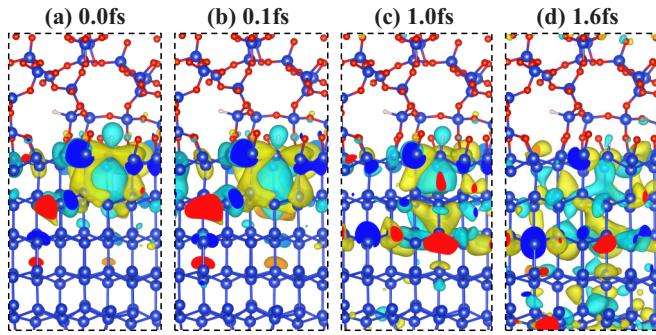


FIG. 3. The evolution of the localized nonadiabatic Si-H state after electron injection.

in which  $\lambda$  is the Lagrange multiplier, and the second term is to ensure the normalization of the coefficients. Consequently,  $\lambda$  and  $C_i$  can be obtained by solving the following eigenstate equation:

$$\sum_j \left[ \int \omega_c(r) \varphi_i(r) \varphi_j(r) dr \right] C_j = \lambda C_i. \quad (8)$$

The eigenvector  $C_i$  that corresponds to the largest eigenvalue  $\lambda$  is plugged into Eq. (6) to generate the deconvoluted Si-H state. The results are shown in Figs. 2(d) and 2(e). It is seen that the superposition of the lower (blue) and higher (red) range of eigenstates produces a “lower” and “upper” state that are nearly the same as the two AB states in  $\text{Si}_4\text{H}_{10}$ , as shown in Fig. 1. These results prove that the spread-out mixed states at the Si/SiO<sub>2</sub> interface indeed originate from the coupling of typical Si-H AB states and the bulk Si host states.

Now that the mutation of Si-H states on the Si/SiO<sub>2</sub> interface has been understood, we can check the effect of electron injection on the Si-H bond vibration. First, to see whether electrons can stay at a nonadiabatic localized Si-H state to induce Si-H dissociation, we have developed an approach in the PWmat code to put an excited electron into the nonadiabatic state shown in Fig. 2(d) and to do the subsequent PWmat simulation. The approach can be summarized in five steps.

(1) Construct the nonadiabatic localized Si-H state by combining a range of adiabatic eigenstates following Eq. (6)–(8).

(2) Orthogonalize all the other eigenstates to this localized state, and use them all (denote as  $\{\psi_j\}$ ) as the input of the subsequent TDDFT simulation.

(3) The occupation of the nonadiabatic state is set to be half occupied (one electron).

(4) Generate the initial charge density by using  $\{\psi_j\}$  and the occupation of each state.

(5) Start the TDDFT simulation, and the  $\{\psi_j\}$  will evolve with time and can be traced by Eq. (3).

The simulation results are shown in Fig. 3, and it is found that the localized state evolves into a delocalized one quickly within 2 fs with the majority of the wave-function amplitudes in the bulk Si. This is understandable since the localized state is not an eigenstate, and there are strong couplings of this state to other states in the bulk Si. Thus, even if one electron can be initially excited to a localized nonadiabatic state, it will not induce any Si-H dissociation.

We next try to excite electrons into the most important eigenstates. Here, to maximize the effect of electrons on the

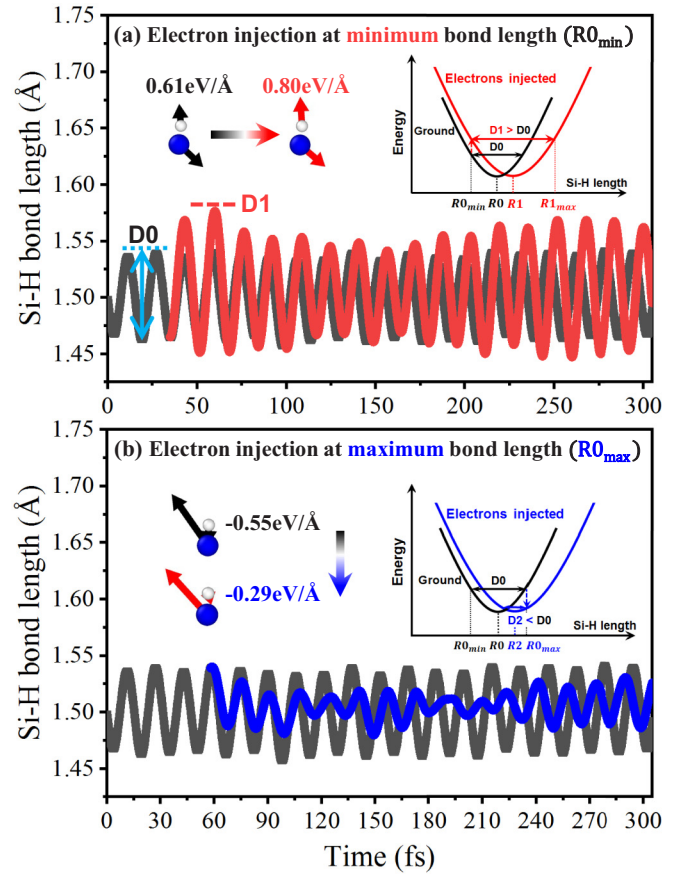


FIG. 4. The Si-H bond dynamics at the Si/SiO<sub>2</sub> interface. Electrons are injected to the Si-H states at (a) 35 fs, when the Si-H bond is at its minimum length, and (b) 58fs, when the bond is at maximum length. The left inset in each subfigure is the force change caused by electrons, and the right inset is a schematic explanation for the phase-coherent and phase-incoherent interaction.

Si-H bond and to represent the MVE, we choose to inject one electron to the 422th state that corresponds to the largest PDOS peak and simultaneously another two electrons to occupy two states nearby. This represents an in-phase injection between different electrons. One alternative approach is to inject three electrons consecutively within the lifetime of the phonon mode. Since the Si-H bond is always vibrating, we decide to choose two extreme time moments to illustrate the time coincidental effects (the phase coherence effect), i.e., when the Si-H bond is shortest and when it is longest. As seen in Fig. 4(a), the electron injection at minimum bond length will enhance the repulsive force between the Si and H atom, and thus the Si-H bond vibration becomes larger in amplitude, which is consistent with the energy accumulation picture of the MVE mechanism. Moreover, it can be seen that the enhanced Si-H vibration can last throughout the simulation, which supports the claim that the Si-H phonon lifetime is long (1–1.5 ns) due to the discrepancy between Si-H stretching frequency and highest bulk Si phonon frequency [31,46]. The temporary decay of vibration shown in Fig. 4(a) around 150 fs is caused by the energy transfer between the stretching mode and bending mode.

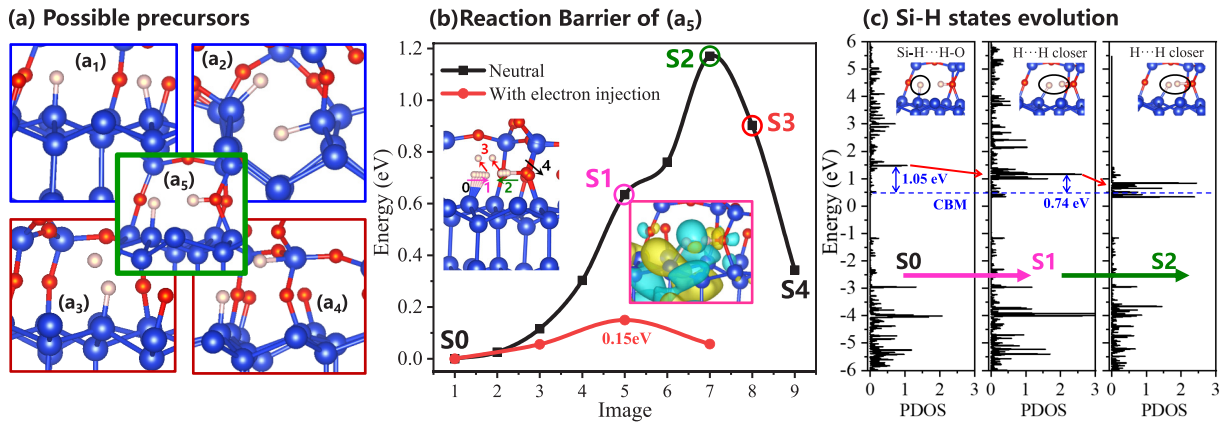


FIG. 5. (a) The precursors that could facilitate Si-H bond breaking. (b) The reaction barrier of the precursor with the “Si-H...H-O” complex. (c) Energy decrease of the Si-H states when the two H atoms approach each other.

The above discussion shows it is impossible to break the Si-H bond by a single electron injection, thus the MVE would be necessary. However, it might still be challenging for the MVE to break a standalone Si-H bond. First, the efficiency of energy transfer between electrons and Si-H bond is very low. If we treat the Si-H bond stretching vibration as completely harmonic, we can calculate the classical potential energy of the oscillator by using  $E = 1/2m\omega^2A^2$ , in which  $m$  is the mass of the H atom, and the  $\omega$  and the amplitude  $A$  can be extracted from TDDFT simulation (Fig. 4). The estimation shows that the original energy is 0.011 eV ( $A = D_0/2$ ), which roughly corresponds to  $1/2 kT$  at room temperature, and it increases to 0.029 eV ( $A = D_1/2$ ) after electron injection. In other words, the energy obtained by the bond is only 0.018 eV, which is rather small compared to the Si-H bond breaking barrier, i.e.,  $\approx 3.6$  eV for stretching break and  $\approx 2.8$  eV for bending break [14]. This is easy to understand since the Si-H states are so strongly coupled with bulk Si states that a large amount of electrons’ energy is given to the bulk Si instead of the local Si-H bond. The limited effect of electron injection on Si-H bond vibration has also been observed in dynamic simulation on Si slabs [12]. Second, the injected electrons could also suppress the Si-H vibration, instead of increasing it, as seen in Fig. 4(b), depending on the phase of oscillation at the moment of electron injection. This is because the occupation of Si-H empty states can only induce repulsive forces to the H atom, and thus it will attenuate the attractive force between H and Si when the two atoms are at their maximum distance. This can also be understood classically from the energy surface change of the Si-H bond, as shown in the inset of Fig. 4. Here, we consider the electron injection as an instantaneous event. After the injection, the energy surface changes from the black curve to the red [Fig. 4(a)] and blue [Fig. 4(b)] curves. As we can see, in Fig. 4(a), the system increases the classical potential energy, while in Fig. 4(b), the system loses the classical potential energy after the injection. This is just a real-time and classical version of Fermi’s “golden rule.” In Fermi’s quantum mechanical “golden rule,” after the transition, the system can gain one phonon like in Fig. 4(a), or lose one phonon like in Fig. 4(b). All this makes the breaking of Si-H bonds extremely challenging, even under the MVE process, which requires an accumulation of many electron

injections with the right phase factor (the energy enhanced phase), within the phonon lifetime of 1–1.5 ns [31].

### C. Assistant effect of the nearby H atom on Si-H bond breaking

Given the aforementioned difficulties to break one standalone Si-H bond, it is natural to wonder whether there are some other structure motifs which are easier to be broken during the device operation. For example, it has been suggested in 2000 that the “Si-OH...H-Si” complex inside SiO<sub>2</sub> could be important to the Si-H bond breaking [13]. For this purpose, we have built multiple possible structures, from which five are shown in Fig. 5(a). The binding energy of H atoms in them follows  $a_1 > a_5 > a_2 > a_3 > a_4$  order. First, it is found that the two kinds of neighboring Si-H bonds ( $a_1$  and  $a_2$ ) are still too stable. The two H atoms prefer to stay far away from each other (3.30 Å at  $a_1$  and 2.06 Å at  $a_2$ ) perhaps due to their negatively charged nature. Second, a free H atom ( $a_3$ ) or a H atom attached to a four-coordinated Si ( $a_4$ ) near the Si-H bond are unstable in the ground state, and they can destroy the Si-H bond without the help of excited electrons. This process should be an important origin of defect creation, but it is not the origin of typical hot (cold) carrier degradation, which happens locally near the drain side and is caused by energetic carriers. In contrast, if one H atom is attached to an O atom ( $a_5$ ) near the Si-H bond, which forms a “Si-H...H-O” complex, the structure will be stable in the electron ground state, and at the same time the two H atoms are close to each other (1.75 Å) for possible reaction. With the participation of the additional H atom, the barrier of the two H atoms to form a H<sub>2</sub> and induce Si-H bond breaking is found to be only 1.17 eV, as shown in Fig. 5(b), and the barrier reduces further after electron injection. Also importantly, as seen in Fig. 5(c), the energy of the unoccupied Si-H states goes down greatly as the two H atoms approach each other (see Fig. S3 in the Supplemental Material [39] for the wave functions), which tremendously benefits the low-energy channel electrons to resonantly tunnel to these states and interact with the Si-H bond. All these structural and electronics properties indicate the important role of surrounding H atoms in Si-H bond breaking.

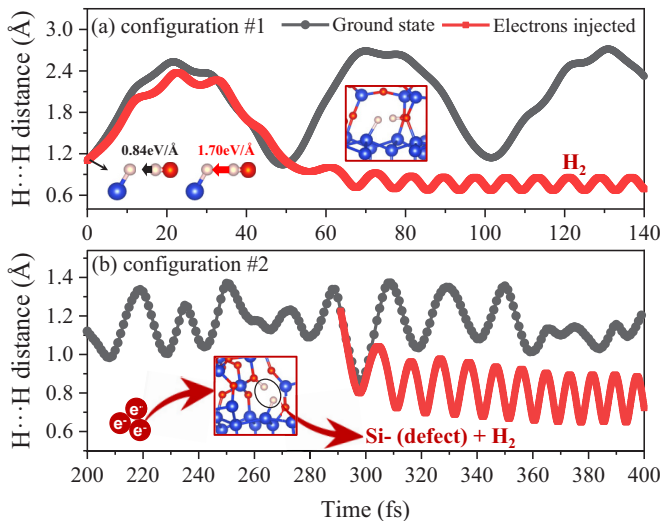


FIG. 6. The carrier induced Si-H bond breaking and  $H_2$  formation in two different Si-H...H-O configurations. The additional H atom bonds with an O atom (a) at the exact Si-SiO<sub>2</sub> interface and (b) inside the amorphous oxide.

It is worth mentioning that the thermal barrier for Si-H bond breaking was experimentally estimated by the simple thermal scheme [5] and generalized simple thermal scheme [9] by using the electron-spin resonance (ESR) technique. The schemes assume that the Si-H bond breaking rate can be expressed by the function of a single-value activation energy (thermal barrier), and the barrier is fitted to be 2.5–2.8 eV, which seems to contradict our simulation results. However, there are a few factors which make it impossible to rule out our hypothesis. First, our neutral system calculation for the barrier of Si-H...H-O is based on the fact that there is an electron in the conduction-band minimum (CBM), which is taken by the reactant after the reaction. On the other hand, the above experiments are done with *p*-type material, where there is no such electron. So, in order for Si-H...H-O to break thermally, one has to first excite one electron from valence-band maximum to CBM (1.13 eV energy), then overcome the barrier of 1.17 eV as we calculated. So, the total barrier will be 2.3 eV, which is not so far away from the experimental value. Second, indeed the simple Si-H center barrier (2.8–3.6 eV [14]) might well be the one measured by the ESR experiment, but this does not prove that the device degradation center (which is broken by channel electrons) is this thermally broken center. For example, it might be possible, in the device considered, that there are many simple Si-H centers, but only a small percentage of Si-H...H-O centers, and as a result the ESR is not sensitive enough to probe that center in the thermal experiment.

With this preanalysis, a demonstration using TDDFT for the dynamic process is imperative. To make it more general, we construct two different configurations that both belong to the Si-H...H-O complex category. In the first configuration, the additional H atom attaches itself to an O atom at exactly the Si-SiO<sub>2</sub> interface, while in the second configuration the H atom bonds with an O atom inside the amorphous oxide (see the insets of Fig. 6). For the first configuration, we start the

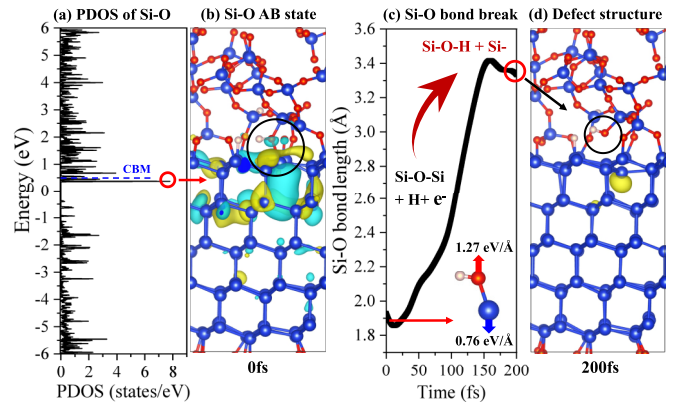


FIG. 7. The Si-O bond breaking caused by the H atom and low-energy electron. (a), (b) The H atom induced Si-O antibonding state. (c) The electron induced repulsive force and bond breaking. (d) The resulted interface defect.

excitation simulation directly from the structure S1 shown in Fig. 5(b), with three extra electrons injected to the Si-H states that correspond to the main PDOS peaks shown in Fig. 5(c). For the second configuration, we first put the structure at 350 K to perform an *ab initio* molecular dynamics to prove its stability, and then introduce three electrons at 291 fs to see their effect. For both cases, as shown in Fig. 6, the injected electrons will enhance the attraction force between the two H atoms greatly, and finally cause the breaking of Si-H bond and O-H bond, and the formation of a  $H_2$  molecule. A Si dangling bond defect is then generated after this reaction. A video of these processes is provided in the Supplemental Material [39].

#### D. The breaking of the interface Si-O bond

The additional H atom not only affects the strength of the Si-H bond, but also weakens the Si-O bond that bridges bulk Si and SiO<sub>2</sub>. As is seen in Figs. 7(a) and 7(b), the attachment of a hydrogen atom on the interface oxygen atom will induce a Si-O antibonding state, the energy level of which is very close to the silicon CBM. This state is already half occupied originally, thus we only inject one more electron to the state to see the effect on Si-O bond vibration. As shown in Fig. 7(c), a large repulsive force is produced on both the O and Si atom by the injected electron, and the Si-O bond breaks soon with the silicon atom sinking into the bulk lattice. A dangling bond defect is thus created as is shown in Fig. 7(d). With the attached H atom, such a Si-O bond breaking process does not require high-energy carriers or multiple carrier interactions, and thus is much easier to happen than the breaking of a Si-H bond. However, it has not been revealed as an important origin of Si/SiO<sub>2</sub> interface degradation before due to the tacit focus on interface Si-H bond breaking, even though hydrogens have been reported to be able to break strained Si-O bonds in amorphous SiO<sub>2</sub> [47–48]. These results suggest that it is important to take both Si-H and Si-O bond breaking into consideration when analyzing interface trap generation and predicting interface state density.



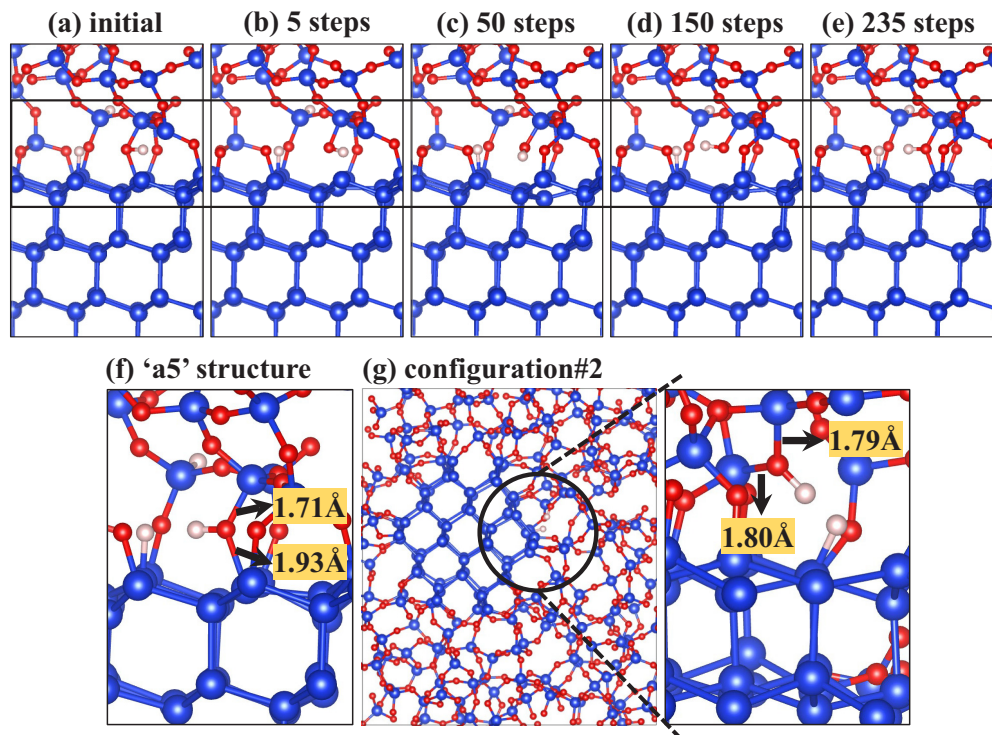


FIG. 8. (a)–(e) The structural relaxation of the  $a_5$  structure after rotating the attached H atom to the other side of the O atom. (f), (g) The Si-O bond detail in the two kinds of Si-H...H-O configurations.

## E. Discussions

### 1. The structural stability of the Si-H...H-O configurations

We have considered two kinds of Si-H...H-O configurations, i.e., the  $a_5$  structure shown in Fig. 5(a) and configuration #2 shown in Fig. 6(b). The full model of configuration #2 is shown in Fig. 8(g). Both the two kinds of configurations are fully relaxed. For the  $a_5$  structure, we manually rotate the attached H atom to the other side of the O atom, as is seen in Fig. 8(a), and then relax it to see whether  $a_5$  is in the global energy minimum. Figures 8(b)–8(e) show the relaxation process, and it can be seen that the attached H atom rotates back after 235 steps, and the system becomes exactly the  $a_5$  structure. This proves that the  $a_5$  configuration is indeed stable. See Fig. S4 in the Supplemental Material [39] for further confirmation of the stability. Nevertheless, we find that the Si-O bond near the  $\text{SiO}_2$  part is 1.71 Å while the one near the bulk Si is 1.93 Å, indicating that the lower bond is not strong. For configuration #2, as is seen in Fig. 8(g), the two Si-O bonds are both  $\approx 1.8$  Å, indicating that the asymmetric strain is small and the configuration is more stable.

We notice that the  $a_5$  configuration is quite similar to the  $[\text{SiO}_4/\text{H}]^0$  center found in bulk  $\text{SiO}_2$  and reported in Ref. [48]. The center also contains a H atom attached to an O atom, and results in two Si-O bonds with asymmetric strength. The difference is that the central Si atom in the  $[\text{SiO}_4/\text{H}]^0$  center bonds with four O atoms as it is inside the  $\text{SiO}_2$ , while the central Si atom in the  $a_5$  structure bonds with one O atom and three Si atoms as it is in the Si/ $\text{SiO}_2$  interface. The O-Si-O angle in the  $[\text{SiO}_4/\text{H}]^0$  center is reported to be as large as  $\approx 165^\circ$ , while the O-Si-Si and Si-Si-Si angles in the  $a_5$  structure are all less than  $119^\circ$ . Moreover,

there is an interface Si-H bond near the O-H bond in the  $a_5$  structure.

We now argue that the formation of Si-H...H-O configurations could be natural during the hydrogen passivation annealing process. When the hydrogen is used to passivate the Si dangling bond, the  $\text{H}_2$  molecule is introduced. Due to the high porosity of  $\text{SiO}_2$ , the  $\text{H}_2$  molecule can diffuse into the system. When it encounters a Si dangling bond, the  $\text{H}_2$

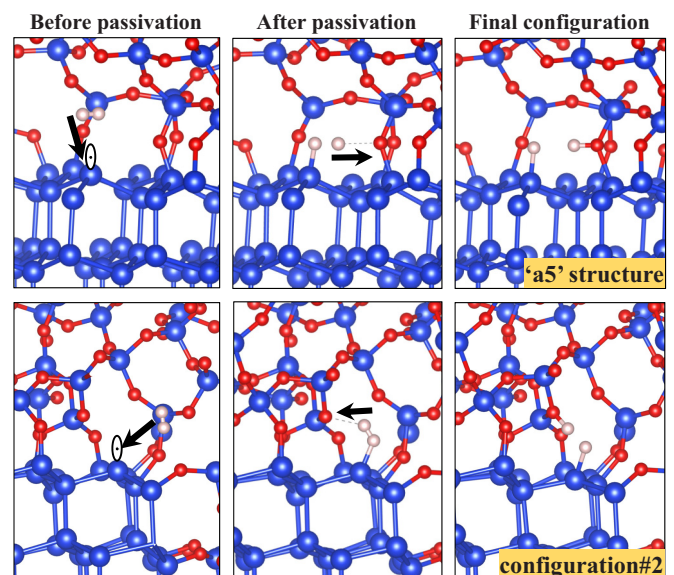


FIG. 9. The extrapolated forming process of the Si-H...H-O complex during hydrogen annealing.

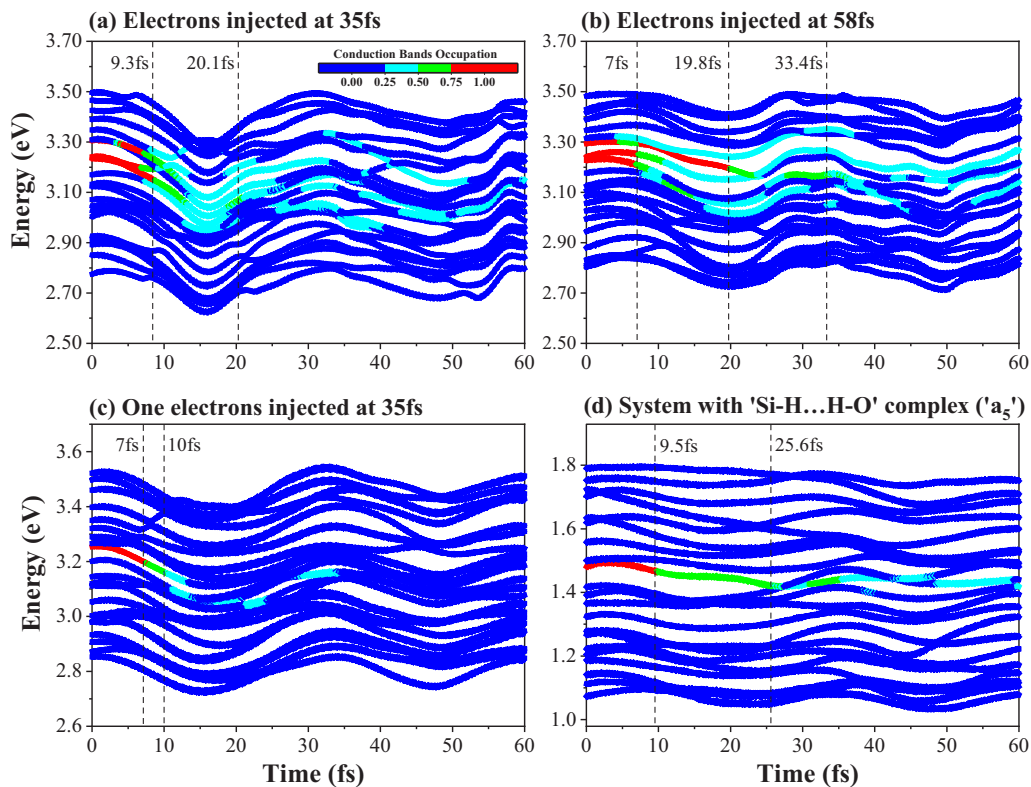


FIG. 10. (a), (b) The retention time of the electrons injected to Si-H antibonding states at different time points (corresponds to Fig. 4). (c), (d) The retention time of the single electron injected to different configurations.

molecule will dissociate, with one H bonding to Si and the leftover H moving towards and bonding to a nearby O in the Si-O-Si bond, hence forming the Si-H...H-O structure. This whole process is shown in Fig. 9. We note that one electron is transferred to the Si CBM when the Si-H...H-O configuration forms under neutral conditions, which means that the Si-H...H-O center is a +1 center. The Hirshfeld charge analysis shows that the additional H atom is slightly (0.14) positively charged.

## 2. The retention time of electrons at Si-H antibonding states

The time length that an electron can stay at the Si-H antibonding states so as to interact with the Si-H bond is an important factor that affects the energy accumulation at the bonds. Therefore, we checked the retention time of the electrons injected to the Si-H states of the Si/SiO<sub>2</sub> interface structure at 35 and 58 fs (corresponds to Fig. 4). As is seen in Figs. 10(a) and 10(b), the electrons can stay at their original states for as long as 9.3 and 19.8 fs depending on the injection time. Such a retention time is not comparable to the Si-H phonon lifetime (1–1.5 ns), but it shows that the injected electrons will not escape from the Si-H antibonding state instantly. We also simulate the case that only one electron is injected to the Si-H antibonding state, and the case that the Si-H...H-O complex exists (*a*<sub>5</sub> structure). For the system with a normal isolated Si-H bond, as is seen in Fig. 10(c), the electron decays from the initial Si-H antibonding state within 7–10 fs, while for the system with Si-H...H-O complex the time is 9.5–25.6 fs, which is a bit longer.

Overall, the electron retention times are short due to the delocalization feature of the Si-H states. It is difficult to retain the electron unless it forms some polaronlike structure. However, since the Si-H antibonding state is in the middle of the conduction bands and hybridizing with other bands, it is impossible to form any polaronlike localized state. However, it is worth noticing that the multiple vibrational excitation mechanism does not demand the interaction of several electrons with the Si-H bond simultaneously, but requires that many electrons interact with the bond successively (one by one) within the lifetime of the excited Si-H bond vibration. The transferred energy from a single electron can reserve at the Si-H bond for a period of 1–1.5 ns even if the electron decays away rapidly. In our simulation, we simplify the successive injection-decay process by injecting three electrons (the ratio to the original total electrons is 3/698≈0.43%) directly, but that should not be a necessary condition for the bond breaking in real devices.

## 3. About the MVE mechanism

The TDDFT simulation results in this paper basically support the MVE mechanism. The first reason is that electron injection can indeed give an amount of energy to the Si-H bond. The second reason is that one single electron cannot break the Si-H bond even in the Si-H...H-O configurations. However, we argue that the MVE mechanism is difficult to succeed for a normal standalone Si-H bond. First, the main antibonding state of a normal Si-H bond is high in energy (≈2.7 eV above CBM in this paper, and ≈3.67 eV above CBM in Ref. [31]), which means that the tunneling probability of



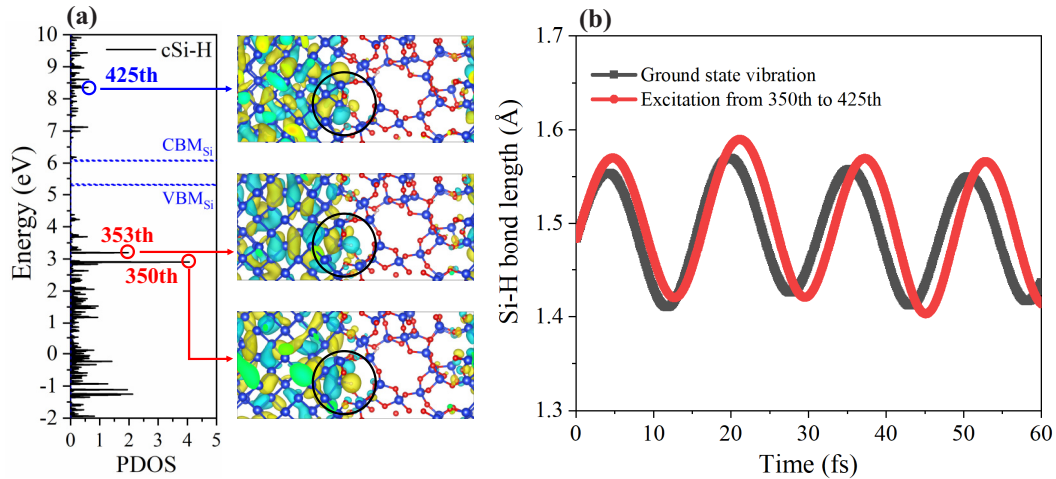


FIG. 11. The simulation on a Si(100) interface structure. (a) The delocalized Si-H states. (b) The small effect of single electron excitation on the bond vibration.

channel electrons to the Si-H states is very low (since the channel electron near the drain side of the device is only about 1 eV above the CBM). Second, even if the electron transfers to the Si-H state (delocalized), the energy it can give to the Si-H bond is only about 0.018 eV, which is too small compared to the bond dissociation barrier of  $\approx 3$  eV. In contrast, as is shown in Fig. 5, the existence of an additional H atom not only can lower the energy level of the Si-H states, and hence facilitate the resonant injection, but it also reduces the Si-H bond dissociation barrier, and thus makes the MVE mechanism more likely to work.

#### 4. The effect of silicon orientation

We mainly presented the study on a Si(111)/SiO<sub>2</sub> interface because the Si dangling bond at the Si(111)/SiO<sub>2</sub> interface is the widely known  $P_b$  center, and the passivation of it by a H atom forms a Si-H bond that well resembles the top Si-H bond of a Si<sub>4</sub>H<sub>10</sub> small cluster, thus we can compare their electronic states and Si-H bond vibration directly. In contrast, the Si atoms at the Si(100)/SiO<sub>2</sub> interface usually bond with two O atoms and another two Si atoms. Therefore, if one O atom is missing and the Si dangling bond is passivated with a H atom, it will form a passivated  $P_{b1}$  center, in which the center Si atom bonds with one H atom, one O atom, and two other Si atoms. Such a local configuration cannot be compared with a Si<sub>4</sub>H<sub>10</sub> cluster directly. Nevertheless, we also studied the Si(100)/SiO<sub>2</sub> interface to see whether the effect of orientation is significant. It can be seen from Fig. 11(a) that the Si-H states, especially the antibonding states, are very delocalized, which is consistent with the results of the Si(111)/SiO<sub>2</sub> interface. Since the antibonding state (425th) is so delocalized, there is no doubt that the electron injection alone will not work. Therefore, we simulate the case that one electron is excited from the bonding state (350th) to the 425th state (although this is not likely to happen in MOSFETs). Even so, the bond vibration is enhanced very slightly, indicating that a normal isolated Si-H bond is really difficult to be broken by carriers alone.

#### 5. The Si-H bond breaking mechanisms in different systems

As shown in Figs. 1 and 11, a single electron excitation is effective in breaking the Si-H bond of a small cluster, but not able to damage the Si-H bond at a Si/SiO<sub>2</sub> interface. The key reason is that the Si-H state in the Si/SiO<sub>2</sub> interface system is too delocalized. Such limited effect of electron excitation on Si-H bond vibration has also been theoretically observed in Si(111) slab systems [12] and bulk SiO<sub>2</sub> systems [13]. However, there are plenty of experiments showing that the Si-H bonds at the Si(111) surface can be dissociated by the electrons/holes injected from a STM tip [15–17], which seems contradictive to the theoretical studies. Our opinion is that the approaching of the STM tip to the H atoms at the Si(111) surface could induce some localized Si-H states, as also proposed in Ref. [12], and the current injection in a STM tip might be much stronger than the theoretical simulation case, and there could also be interactions between many H atoms at the Si(111) surface. For the Si-H bond breaking in semiconductor-oxide interfaces of MOSFETs, there are several experimental works indicating that the mechanism is beyond the only interaction of electrons and Si-H bonds. First, the carrier degradation in MOSFETs is still severe even if the source-drain operation voltage is reduced to  $\approx 1$  eV [22], but the energy difference between Si CBM to the main Si-H states is found to be  $\approx 2.7$  eV as seen in Fig. 2, and is reported to be  $\approx 3.67$  eV on average by Jech *et al.* [31]. Although the electron-electron scattering might result in some carriers with such high energy, the probability is small, by a corresponding Boltzmann distribution factor. Second, it has been demonstrated that the blocking of hydrogen and water from entering the MOSFETs is effective in relieving hot carrier degradation [49], indicating the possible role of the H atom and hydroxyl (-OH) in defect creation.

## IV. CONCLUSIONS

In summary, the dynamical process of defect creation induced by low-energy carriers has been investigated using *ab initio* TDDFT simulations on realistic Si/SiO<sub>2</sub> interfaces. We

have two main conclusions through our paper: first, we show that it is almost impossible to break the Si-H bond in a single electron event, thus multiple electron events (MVE mechanism) are necessary. This is in agreement with the common belief in the community, but our paper demonstrated it from an angle of real-time simulations. Second, we found that the most possible configuration for Si-H bond breaking is a Si-H $\cdots$ H-O complex, which is likely to be formed during the hydrogen passivation annealing process. While a standalone Si-H bond is very stable due to its higher energy level and delocalized nature of the Si-H AB state, the bond in the Si-H $\cdots$ H-O complex is much more vulnerable. This is mostly because its eigenstate is more localized than that of the standalone Si-H bond, and its state energy is lower than the Si-H bond, which makes it easier for electron injection from the channel. Lastly, its energy barrier for dissociation is much lower than normal Si-H due to the possibility to form an H<sub>2</sub> molecule after the reaction. Thus, overall, we propose the Si-H $\cdots$ H-O-like structure could be the culprit for defect creation and device degradation. Our theoretical hypothesis awaits experimental verification. If this hypothesis is proved to be correct, one can think about new ways to improve the device, e.g., by removing Si-H $\cdots$ H-O centers while keeping the Si-H center. How one

can do that should be subjects for future study. Perhaps this can be done with some special thermal treatment, or chemical treatment (e.g., chemical species strong enough to react with the H in H-O, but not with the H in Si-H). While our main goal for the current paper is to focus on the mechanism of the degradation, rather than come up with the actual techniques to mitigate the problem, a clear understanding could be the first step towards device improvements.

#### ACKNOWLEDGMENTS

This work was supported by National Natural Science Foundation of China (Grants No. 61927901, No. 12004375, No. 11774338, No. 11574304, No. 12025407, and No. 91850120), China Key Research and Development Program (Grant No. 2018YFA0306101), Chinese Academy of Sciences (CAS)–Peking University Pioneer Cooperation Team, the Youth Innovation Promotion Association of CAS (Grant No. 2016109), and CAS Grant No. 6J6011000. L.-W.W. was supported through the Basic Energy Sciences program of the Office of Science of the U.S. Department of Energy under Grant No. DE-SC0004993 under the Theory of Material program.

- 
- [1] T. Grasser, *Hot Carrier Degradation in Semiconductor Devices* (Springer, New York, 2014).
- [2] R. B. Fair and R. C. Sun, Threshold voltage instability in MOSFET's due to channel hot hole emission, in *Proceedings of the IEEE International Electron Devices Meeting (IEDM)*, (IEEE, Washington, DC, USA, 1980), pp. 746–749.
- [3] Z. Chen, K. Hess, J. Lee, J. W. Lyding, E. Rosenbaum, I. Kizilyalli, and S. Chetlur, Mechanism for hot-carrier-induced interface trap generation in MOS transistors, in *Proceedings of the IEEE International Electron Devices Meeting (IEDM)*, (IEEE, Washington, DC, USA, 1999), pp. 85–88.
- [4] S. Mahapatra, *Fundamentals of Bias Temperature Instability in MOS Transistors* (Springer, New York, 2016).
- [5] K. L. Brower and S. M. Myers, Chemical kinetics of hydrogen and (111) Si-SiO<sub>2</sub> interface defects, *Appl. Phys. Lett.* **57**, 162 (1990).
- [6] C. G. Van de Walle, Energies of various configurations of hydrogen in silicon, *Phys. Rev. B* **49**, 4579 (1994).
- [7] B. Tuttle and C. G. Van de Walle, Structure, energetics, and vibrational properties of Si-H bond dissociation in silicon, *Phys. Rev. B* **59**, 12884 (1999).
- [8] B. Tuttle, Energetics and diffusion of hydrogen in SiO<sub>2</sub>, *Phys. Rev. B* **61**, 4417 (2000).
- [9] A. Stesmans, Dissociation kinetics of hydrogen-passivated  $P_b$  defects at the (111)Si/SiO<sub>2</sub> interface, *Phys. Rev. B* **61**, 8393 (2000).
- [10] C. G. Van de Walle and B. R. Tuttle, Microscopic theory of hydrogen in silicon devices, *IEEE Trans. Electron Devices* **47**, 1779 (2000).
- [11] S. N. Rashkeev, D. M. Fleetwood, R. D. Schrimpf, and S. T. Pantelides, Defect Generation by Hydrogen at the Si-SiO<sub>2</sub> Interface, *Phys. Rev. Lett.* **87**, 165506 (2001).
- [12] Y. Miyamoto and O. Sugino, First-principles electron-ion dynamics of excited systems: H-terminated Si(111) surfaces, *Phys. Rev. B* **62**, 2039 (2000).
- [13] A. Yokozawa and Y. Miyamoto, Hydrogen dynamics in SiO<sub>2</sub> triggered by electronic excitations, *J. Appl. Phys.* **88**, 4542 (2000).
- [14] M. Jech, A.-M. El-Sayed, S. Tyaginov, A. L. Shluger, and T. Grasser, Ab initio treatment of silicon-hydrogen bond rupture at Si/SiO<sub>2</sub> interfaces, *Phys. Rev. B* **100**, 195302 (2019).
- [15] T.-C. Shen, C. Wang, G. C. Abeln, J. R. Tucker, J. W. Lyding, Ph. Avouris, and R. E. Walkup, Atomic-scale desorption through electronic and vibrational excitation mechanisms, *Science* **268**, 1590 (1995).
- [16] Ph. Avouris, R. E. Walkup, A. R. Rossi, T.-C. Shen, G. C. Abeln, J. R. Tucker, and J. W. Lyding, STM-induced H atom desorption from Si(100): Isotope effects and site selectivity, *Chem. Phys. Lett.* **257**, 148 (1996).
- [17] K. Stokbro, C. Thirstrup, M. Sakurai, U. Quaade, B. Y. K. Hu, F. Perez-Murano, and F. Grey, STM-Induced Hydrogen Desorption Via a Hole Resonance, *Phys. Rev. Lett.* **80**, 2618 (1998).
- [18] D. S. Lin and R. P. Chen, Hydrogen-desorption kinetic measurement on the Si(100)-2  $\times$  1: H surface by directly counting desorption sites, *Phys. Rev. B* **60**, R8461(R) (1999).
- [19] E. T. Foley, A. F. Kam, J. W. Lyding, and P. Avouris, Cryogenic UHV-STM Study of Hydrogen and Deuterium Desorption from Si(100), *Phys. Rev. Lett.* **80**, 1336 (1998).
- [20] J. E. Chung, M. C. Jeng, J. E. Moon, P. K. Ko, and C. M. Hu, Low-voltage hot-electron currents and degradation in deep-submicrometer MOSFETs, *IEEE Trans. Electron Devices* **37**, 1651 (1990).

- [21] S. Aur, Low-voltage hot carrier effects and stress methodology, in *Proceedings of the Symposium on VLSI Technology Digest*, (IEEE, Taipei, Taiwan, 1995), pp. 277–280.
- [22] G. La Rosa and S. E. Rauch, Channel hot carrier effects in n-MOSFET devices of advanced submicron CMOS technologies, *Microelectron. Reliab.* **47**, 552 (2007).
- [23] M. V. Fischetti and S. E. Laux, Monte Carlo study of sub-band-gap impact ionization in small silicon field-effect transistors, in *Proceedings of the IEEE International Electron Devices Meeting (IEDM)*, (IEEE, Washington, DC, USA, 1995), pp. 305–308.
- [24] P. A. Childs and C. C. C. Leung, A one dimensional solution of the Boltzmann transport equation including electron-electron interactions, *J. Appl. Phys.* **79**, 222 (1996).
- [25] S. E. Rauch, G. La Rosa, and F. J. Guarin, Role of EE scattering in the enhancement of channel hot carrier degradation of deep-submicron NMOSFETs at high  $V_{GS}$  conditions, *IEEE Trans. Device Mater. Reliab.* **1**, 113 (2001).
- [26] K. Hess, L. F. Register, B. Tuttle, J. Lyding, and I. C. Kizilyalli, Impact of nanostructure research on conventional solid-state electronics: The giant isotope effect in hydrogen desorption and CMOS lifetime, *Physica E* **3**, 1 (1998).
- [27] Z. Chen, P. Ong, A. K. Mylin, V. Singh, and S. Chetlur, Direct evidence of multiple vibrational excitation for the Si-H/D bond breaking in metal-oxide-semiconductor transistors, *Appl. Phys. Lett.* **81**, 3278 (2002).
- [28] C. Guerin, V. Huard, and A. Bravaix, General framework about defect creation at the Si/SiO<sub>2</sub> interface, *J. Appl. Phys.* **105**, 114513 (2009).
- [29] S. Tyaginov, M. Bina, J. Franco, D. Osintsev, O. Triebl, B. Kaczer, and T. Grasser, Physical modeling of hot-carrier degradation for short- and long-channel MOSFETs, in *Proceedings of the IEEE International Reliability Physics Symposium*, (IEEE, Waikoloa, HI, USA, 2014), pp. XT.16.1–XT.16.8.
- [30] A. Bravaix, C. Guerin, V. Huard, D. Roy, J. M. Roux, and E. Vincent, Hot-carrier acceleration factors for low power management in DC-AC stressed 40 nm NMOS node at high temperature, in *Proceedings of the IEEE International Reliability Physics Symposium*, (IEEE, Montreal, QC, Canada, 2009), pp. 531–548.
- [31] M. Jech, S. Tyaginov, B. Kaczer, J. Franco, D. Jabs, C. Jungemann, M. Walth, and T. Grasser, First-principles parameter-free modeling of n- and p-FET hot-carrier degradation, in *Proceedings of the IEEE International Electron Devices Meeting (IEDM)*, (IEEE, San Francisco, CA, USA, 2019), pp. 24.1.1–24.1.4.
- [32] S. Mahapatra and U. Sharma, A review of hot carrier degradation in n-Channel MOSFETs—Part I: Physical mechanism, *IEEE Trans. Electron Devices* **67**, 2660 (2020).
- [33] Z. Wang, S. S. Li, and L. W. Wang, Efficient Real-Time Time-Dependent Density Functional Theory Method and Its Application to a Collision of an Ion with a 2D Material, *Phys. Rev. Lett.* **114**, 063004 (2015).
- [34] J. Ren, N. Vukmirović, and L. W. Wang, Nonadiabatic molecular dynamics simulation for carrier transport in a pentathiothene butyric acid monolayer, *Phys. Rev. B* **87**, 205117 (2013).
- [35] W. Jia, Z. Cao, L. Wang, J. Fu, X. Chi, W. Gao, and L. W. Wang, The analysis of a plane wave pseudopotential density functional theory code on a GPU machine, *Comput. Phys. Comm.* **184**, 9 (2013).
- [36] W. Jia, J. Fu, Z. Cao, L. Wang, X. Chi, W. Gao, and L. W. Wang, Fast plane wave density functional theory molecular dynamics calculations on multi-GPU machines, *J. Comput. Phys.* **251**, 102 (2013).
- [37] M. Schlipf and F. Gygi, Optimization algorithm for the generation of ONCV pseudopotentials, *Comput. Phys. Commun.* **196**, 36 (2015).
- [38] F. Zheng, H. H. Pham, and L.-W. Wang, Effects of the c-Si/a-SiO<sub>2</sub> interfacial atomic structure on its band alignment: An ab initio study, *Phys. Chem. Chem. Phys.* **19**, 32617 (2017).
- [39] See Supplemental Material at <http://link.aps.org/supplemental/10.1103/PhysRevB.104.115310> for the verification of Si-H electronic states by HSE functional, the effect of bond elongation on Si-H states, the wave-function evolution induced by H approaching, the structural stability confirmation, and the videos of Si-H bond breaking simulated by TDDFT.
- [40] P. Guyot-Sionnest, P. H. Lin, and E. M. Hiller, Vibrational dynamics of the Si-H stretching modes of the Si(100)/H:2 × 1 surface, *J. Chem. Phys.* **102**, 4269 (1995).
- [41] Y. Y. Liu, F. Zheng, X. Jiang, J. W. Luo, S. S. Li, and L. W. Wang, Ab initio investigation of charge trapping across the crystalline-Si–amorphous-SiO<sub>2</sub> interface, *Phys. Rev. Appl.* **11**, 044058 (2019).
- [42] A.-M. El-Sayed, M. B. Watkins, V. V. Afanas'ev, and A. L. Shluger, Nature of intrinsic and extrinsic electron trapping in SiO<sub>2</sub>, *Phys. Rev. B* **89**, 125201 (2014).
- [43] Y. Y. Liu, and X. Jiang, Physics of hole trapping process in high-k gate stacks: A direct simulation formalism for the whole interface system combining density-functional theory and Marcus theory, in *Proceedings of the IEEE International Electron Devices Meeting (IEDM)* (IEEE, San Francisco, CA, USA, 2018), pp. 40.1.1–40.1.4.
- [44] Y. Y. Liu, F. Liu, R. Wang, J. W. Luo, X. Jiang, R. Huang, S. S. Li, and L. W. Wang, Characterizing the charge trapping across crystalline and amorphous Si/SiO<sub>2</sub>/HfO<sub>2</sub> stacks from first-principle calculations, *Phys. Rev. Appl.* **12**, 064012 (2019).
- [45] B. Kaduk, T. Kowalczyk, and T. Van Voorhis, Constrained density functional theory, *Chem. Rev.* **112**, 321 (2012).
- [46] I. Andrianov and P. Saalfrank, Theoretical study of vibration-phonon coupling of H adsorbed on a Si(100) surface, *J. Chem. Phys.* **124**, 034710 (2006).
- [47] A.-M. El-Sayed, M. B. Watkins, T. Grasser, V. V. Afanas'ev, and A. L. Shluger, Hydrogen-Induced Rupture of Strained Si-O Bonds in Amorphous Silicon Dioxide, *Phys. Rev. Lett.* **114**, 115503 (2015).
- [48] A.-M. El-Sayed, Y. Wimmer, W. Goes, T. Grasser, V. V. Afanas'ev, and A. L. Shluger, Theoretical models of hydrogen-induced defects in amorphous silicon dioxide, *Phys. Rev. B* **92**, 014107 (2015).
- [49] S. Yoshida, K. Okuyama, F. Kanai, Y. Kawate, M. Motoyoshi, and H. Katto, Improvement of endurance to hot carrier degradation by hydrogen blocking P-SiO, in *Proceedings of the IEEE International Electron Devices Meeting (IEDM)* (IEEE, San Francisco, CA, USA, 1988), pp. 22–25.